AIP | The Journal of Chemical Physics

Collisional and photoinitiated reaction dynamics in the ground electronic state of Ca–HCl

Cristina Sanz, Ad van der Avoird, and O. Roncero

Citation: J. Chem. Phys. **123**, 064301 (2005); doi: 10.1063/1.1995700
View online: http://dx.doi.org/10.1063/1.1995700
View Table of Contents: http://jcp.aip.org/resource/1/JCPSA6/v123/i6
Published by the American Institute of Physics.

Collisional and photoinitiated reaction dynamics in the ground electronic state of Ca–HCl

Cristina Sanz
Instituto de Matemáticas y Física Fundamental, Consejo Superior de Investigaciones Científicas (CSIC), Serrano 123, 28006 Madrid, Spain

Ad van der Avoird
Institute of Theoretical Chemistry, Institute for Molecules and Materials (IMM), Radboud University, Nijmegen, Toernooiveld 1, 6525 ED Nijmegen, The Netherlands

O. Roncero[a)]
Instituto de Matemáticas y Física Fundamental, Consejo Superior de Investigaciones Científicas (CSIC), Serrano 123, 28006 Madrid, Spain

(Received 22 April 2005; accepted 16 June 2005; published online 12 August 2005)

Ca+HCl(v,j) reactive collisions were studied for different rovibrational states of the HCl reactant using wave-packet calculations in reactant Jacobi coordinates. A recently proposed potential-energy surface was used with a barrier of ≈0.4 eV followed by a deep well. The possibility of an insertion mechanism due to this last well has been analyzed and it was found that once the wave packet passes over the barrier most of it goes directly to CaCl+H products, which shows that the reaction dynamics is essentially direct. It was also found that there is no significant change in the reaction efficiency as a function of the initial HCl rovibrational state, because CaHCl at the barrier has an only little elongated HCl bond. Near the threshold for reaction with HCl(v=0), however, the reaction shows significant steric effects for $j>0$. In a complementary study, the infrared excitation from the Ca–HCl van der Waals well was simulated. The spectrum thus obtained shows several series of resonances which correspond to quasibound states correlating to excited HCl(v) vibrations. The Ca–HCl binding energies of these quasibound states increase dramatically with v, from 75 to 650 cm^{-1}, because the wave function spreads increasingly over larger HCl bond lengths. Thus it explores the region of the barrier saddle point and the deep insertion well. Although also the charge-transfer contribution increases with v, the reaction probability for resonances of the v=2 manifold, which are well above the reaction threshold, is still negligible. This explains the relatively long lifetimes of these v=2 resonances. The reaction probability becomes significant at v=3. Our simulations have shown that an experimental study of this type will allow a gradual spectroscopic probing of the barrier for the reaction. © *2005 American Institute of Physics*.
[DOI: 10.1063/1.1995700]

I. INTRODUCTION

The reactive collisions between metal atoms and hydrogen halides constitute excellent models to analyze the influence of the initial state of the reactants and its effect on the final-state distribution. Their study has introduced many of the fundamental concepts nowadays used to interpret reaction dynamics,[1–4] as recently reviewed.[5] Such reactions are envisaged to be governed by the "harpoon" mechanism:[6,7] an electron of the metal atom (M) "jumps" to the halide (HX) and forms an unstable anion HX^-. This ion dissociates, which leads to the formation of ionic M^+X^- products. Theoretically, such a process is interpreted as a crossing of potential curves between covalent diabatic states correlating to reactants and ionic diabatic states correlating to products. When the metal atom M has a single active electron, as in the case of alkali atoms, only one crossing is usually enough to understand the process, which leads to products in a single electronic state. When the metal atom has two active electrons, as in the case of alkali-earth atoms, several electronic states of the metal ion are involved and, therefore, several crossings appear, leading to multiple harpoon mechanisms.[5] In this situation many complicated nonadiabatic processes occur and produce several final electronic states of the products. The electronically excited MX products emit, and many experimental chemiluminescence studies have been devoted to the collision dynamics from the excited electronic states of the reactants.[8–16] An interesting alternative to study such nonadiabatic processes consists of exciting the system from a van der Waals complex formed in the entrance channel of the ground electronic state reaction.[17–20]

The collision reaction dynamics in the ground electronic state has been investigated experimentally for several alkali-earth atoms reacting with different hydrogen halides.[21–29] These studies concerned the effects of the collision energy and initial vibrational excitation of HX, as well as the final rovibrational state distribution of the fragments. Typically, Ca+HX reactions are endoergic, while Ba+HX reactions are

[a)]Electronic mail: oroncero@imaff.cfmac.csic.es

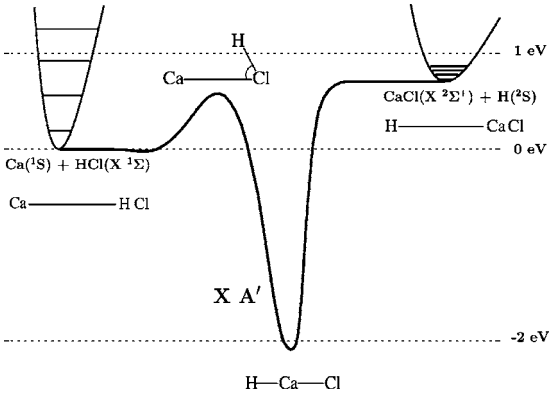

FIG. 1. Minimum-energy path (in eV) for the reaction Ca+HCl→CaCl +H in the ground electronic state. Geometries are shown at each stationary point.

exoergic.[21,29] The ground potential-energy surface (PES) of these systems presents a barrier along the reaction path, followed by a very deep well that corresponds to a linear H*MX* insertion complex stabilized by the divalent character of the alkali-earth atom.[30] These two characteristics may introduce important features in the reaction mechanism. It is interesting to address the question to what extent the reaction is direct, i.e., governed by the barrier, or indirect, i.e., mediated by long-lived resonances due to the deep well of the H*MX* complex.

Obtaining realistic PES's for this type of systems has revealed to be rather difficult, because of large changes in the ionic character along the reaction path. Most PES's are based on semiempirical approaches[31–33] or on models such as the diatomics-in-molecules (DIMs) method.[34,35] PES's based on accurate *ab initio* calculations are more scarce. After the work on Ca+HF by Jaffe *et al.*,[30] it was only recently that accurate PES's have been proposed.[36–38] In this work we shall analyze the reaction dynamics of Ca+HCl on a recent PES for the ground electronic state.[38]

Ca+HCl→CaCl+H is one of the most studied reactions involving an alkali-earth atom and a hydrogen halide. Nearly all the investigations involve the electronic excitation of the Ca atom, and detection of the chemiluminescence of CaCl fragments in the excited *A* or *B* states. Such experiments were performed either with collisions[8–16] or by photoinitiation from the van der Waals complex in the entrance channel.[17–20] Even though in all these studies the system is electronically excited, the formation of CaCl fragments in the ground electronic state seemed to be a major reaction path.[12,20]

The Ca+HCl reaction in the ground electronic state has not been studied before, possibly because it is highly endoergic. This is shown in Fig. 1. Wave-packet calculations of the Ca+HCl(v,j) reactive collisions are presented in this paper. The potential-energy surface of the ground adiabatic electronic state shows features which can be interpreted in terms of the covalent/ionic crossings mentioned above. That is the case, for example, for the barrier in the minimum-energy reaction path in Fig. 1. The excited adiabatic electronic states resulting from the avoided crossings are expected to be at rather high energies. For this reason it is not likely that nonadiabatic transitions will occur at the low collisional energies considered in this work, and the usual Born-Oppenheimer approximation is expected to hold rather well. Therefore, the reactive collisions are studied in the adiabatic ground electronic state. Also, the reaction dynamics after infrared excitation from the van der Waals well is simulated to spectroscopically probe the energy region around the transition state. The paper is organized as follows. Section II contains a brief description of some details of the wave-packet calculation. In Sec. III the results for the reactive collisions are presented, while Sec. IV is devoted to the photoinitiated dynamics. Finally, in Sec. V some conclusions are extracted.

II. DYNAMICAL CALCULATIONS

The reactant Jacobi vectors used in the calculations are the vector **r** pointing from the Cl to the H nucleus and the vector **R** that points from the HCl center of mass to the Ca atom. The components of these vectors are expressed in a body-fixed frame which the three atoms in the xz plane and the z axis parallel to **R**. Three Eulerian angles (ϕ,θ,χ) determine the orientation of the body-fixed axes with respect to a space-fixed frame and three internal variables define the nuclear configuration of the system: r, the internuclear H–Cl distance, R, the modulus of **R**, and the angle γ, with $\cos\gamma = \mathbf{r}\cdot\mathbf{R}/rR$.

Along the Ca+HCl→CaCl+H reaction path shown in Fig. 1 there is an insertion minimum, with the Ca atom in between H and Cl. Sometimes Jacobi coordinates are not well adapted to this situation, because the radial coordinate R may become zero and the Hamiltonian becomes singular. However, this is not the case here, because of the large mass mismatch between Cl and H atoms. The center of mass of the diatom is very close to the Cl nucleus and the PES is strongly repulsive at $R=0$ because of a very large overlap between the Ca and Cl atoms. Contour plots of the PES developed in Ref. 38 are displayed in the top panel of Fig. 2. They clearly show that $R=0$ is excluded in the dynamics.

In the calculations to be described below, the wave packet is expanded as[39–41]

$$\Psi^{JM}(\mathbf{r},\mathbf{R},t)=\left[\frac{2J+1}{8\pi^2}\right]^{1/2}\sum_{\Omega}\frac{\Phi^J_\Omega(r,R,\gamma,t)}{rR}D^J_{M\Omega}(\phi,\theta,\chi)^*, \tag{1}$$

where $D^J_{M\Omega}$ are Wigner rotation matrices.[42] For given total angular momentum J, M and Ω are its projections on the space-fixed and body-fixed z axes, respectively. Given the large reduced mass associated with the end-over-end vector **R**, the Coriolis coupling is small for low J, but rotational barriers in the PES are small as well and require high values of J to converge the cross sections. However, because of the difficulty of performing "exact" quantum simulations, the centrifugal sudden (CS) approach was used here, in which the sum over Ω is restricted to a single value, that of the initial state of the HCl reactant. This approximation is expected to be well suited since in the entrance channel the Jacobi vector **R** nearly coincides with a principal axis of inertia, due to the large mass mismatch between the light **H** atom and the heavy Cl atom. The CS approach was found to

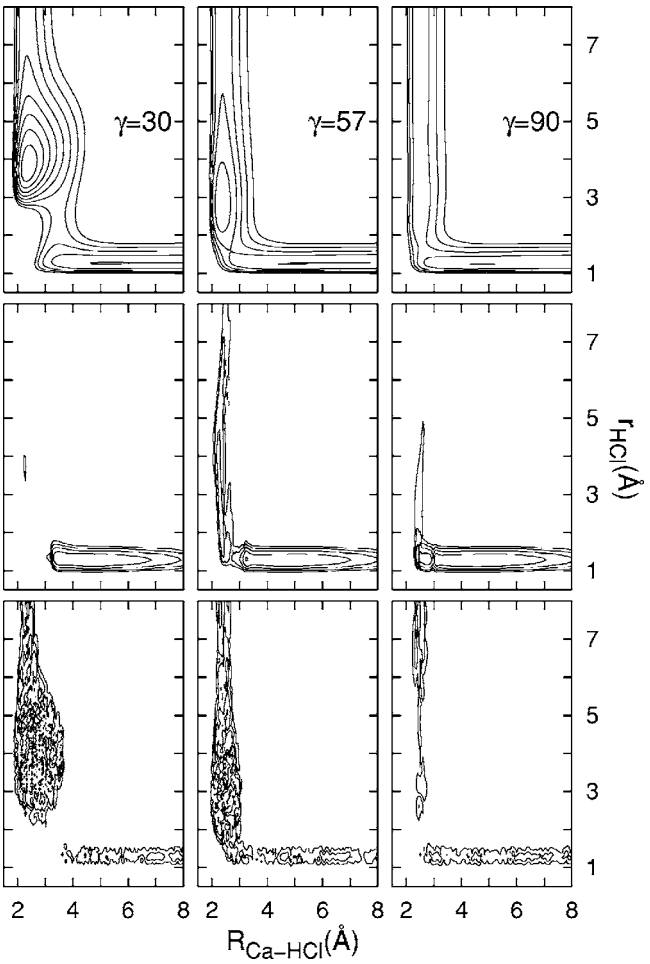

FIG. 2. Contour plots of the CaHCl PES (top panel), and wave packet for the Ca+HCl($v=0,j=0$) reaction with $J=0$ for $t=0.4$ ps (middle panel) and for $t=3$ ps (bottom panel).

work quite well in similar systems, such as Li+HF,[39] even though the latter system is lighter than Ca+HCl and should have a larger Coriolis coupling. Once in the product channel, Coriolis coupling may become more important but if the reaction goes directly to products, the total reaction probability is not sensitive to the final Ω value. Therefore, the major concern regarding the validity of the CS approximation is that the dynamics will be dominated by an indirect mechanism in which the system recrosses over the reaction barrier. This will be analyzed.

The complexity of quantum reaction dynamics on this system is due to the large masses involved, the presence of a high barrier (of $\approx$0.5 eV), and a deep insertion well in the product channel, as can be seen in Fig. 1. All these factors lead to the use of very dense grids covering large nuclear configuration regions to describe the dynamics. The $\Phi^J_\Omega(r,R,\gamma,t)$ coefficients in Eq. (1) are represented in the following grids. The internal coordinates r and R are described by 256×1024 equidistant points, in the intervals $0.07\leqslant r\leqslant 17$ Å and $1.5\leqslant R\leqslant 25$ Å, respectively, while the angle γ is described by 30 Gauss-Legendre quadrature points. In order to avoid problems when the wave packet reaches the edges of the grid, the usual absorption procedure was applied; the wave packet is multiplied by a damping exponential function, $\exp[-\alpha_x(x-x_{\text{abs}})^2]$, with $x=r$ or R and $r_{\text{abs}}=10$ Å, $R_{\text{abs}}=18$ Å. The parameters α_r and α_R were optimized to avoid reflections.

The wave packet is propagated with a Chebyshev propagator,[43,44] using time steps of 2.5 fs. These small steps are required to resolve properties such as reaction probabilities over a large energy range, of $\approx$1 eV. Also, the total time required to converge the different quantities is rather long ($\approx$10 ps in the collisions and even longer in the photoinitiated processes) because of the presence of long-lived resonances. For higher values of J the total time can be considerably reduced because resonances become broader.

The initial wave packet in collision processes is built as an incoming complex Gaussian function multiplied by the initial rovibrational state of the HCl reactant. Body-fixed Bessel functions were used in the CS approach, as described previously.[40,45] The Gaussian wave packet is initially placed at relatively long distances, around $R=16$ Å, because of the long-range character of the PES. In photoinitiated dynamics the initial wave packet is built as described previously.[41,46] It is the product of the electric dipole transition operator and the initial bound-state wave function, which in the present study corresponds to a particular bound van der Waals level in the entrance channel.

The PES used for the dynamics was obtained and described in Ref. 38. In the course of the propagation the reaction probability is obtained using the flux method,[47–50] as implemented for collisions[51] or photodissociation processes.[41] The energy distribution of the final HCl(v,j) rovibrational states is obtained by the method of Balint-Kurti and co-workers.[52,53]

III. REACTIVE COLLISION DYNAMICS

According to the PES the Ca+HCl$\rightarrow$CaCl+H reaction is endoergic by 0.63 eV and has a barrier of 0.55 eV at a HCl bond length slightly elongated from that of isolated HCl. The actual situation is somewhat different, because one has to consider the zero-point energies of HCl, of $\approx$0.19 eV, and of CaCl, of $\approx$0.02 eV, so that the real endoergicity is reduced to 0.46 eV. There is also an effect of the zero-point energy at the saddle point that will be discussed later.

Between the barrier and the products is a deep HCaCl insertion well, see Fig. 1, and it is interesting to determine whether the reaction follows either an insertion or a direct mechanism. In order to get an intuitive insight, the wave packet is shown at different times, $t=0.4$ ps in the middle panel of Fig. 2, and $t=3$ ps in the bottom panel. The reaction occurs in a small angular cone around the saddle point at the barrier. It seems that for short times, once the wave packet has passed over the barrier, it does not notice the deep insertion well and goes directly towards products. At longer times, however, a portion of the wave packet starts exploring the region of the well and gives rise to resonances.

Reaction probabilities obtained for different times, as shown in Fig. 3, corroborate this dynamical picture. At 0.75 ps, which is a relatively short time especially if one realizes that the wave packet needs $\approx$0.35 ps to arrive at the barrier, most of the reaction has occurred. The increase of the

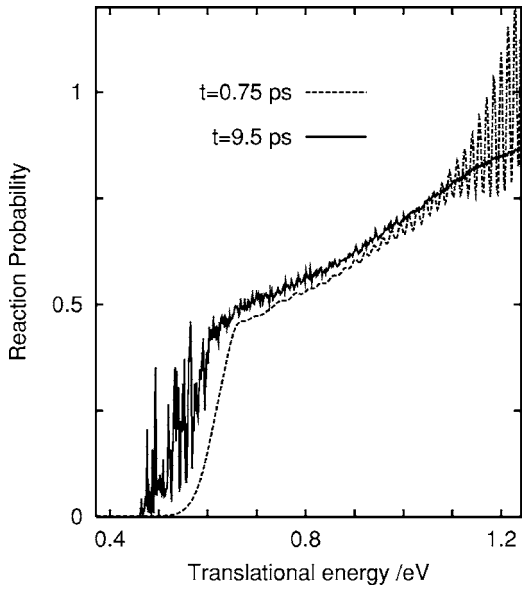

FIG. 3. Reaction probability in Ca+HCl($v=0, j=0$) collisions with $J=0$ for $t=0.75$ and 9.5 ps.

reaction probability that occurs after this time corresponds mostly to narrow resonances associated with the insertion well. It may be concluded that the reaction mechanism is essentially direct, while only few resonances appear due to the insertion well. The role of such resonances is more significant for energies just above the reaction threshold. They may be considered to mark the threshold for the direct reaction mechanism. Therefore, the main reaction mechanism may be considered to be a direct one. In such a situation the CS approximation is expected to work fairly well, as in several direct reactions without potential wells.[54] Near the threshold, however, where resonances play an important role, the CS approach is expected to work less well, as recently found for indirect reactions such as $H^+ + H_2$.[55]

The reaction probability shows a clear threshold at ≈ 0.5 eV, while the saddle point is only 0.36 eV over the HCl($v=0, j=0$) reactants. The difference corresponds to zero-point energy at the saddle point, where the resonances play an important role. Above this threshold, the reaction probability increases slowly in the energy interval considered. The same behavior is found for higher values of J, in Fig. 4. The reaction probabilities for $J>0$ are obtained using the CS approach, and they are very well approximated by the J-shifting approach.[56] There is only a slight decrease in the reaction probability with increasing J.

In order to study the effect of the initial rotation of HCl the same calculations have been performed for Ca+HCl($v=0, j=1$) for several values of J, as shown in Fig. 5. Two families of results, for $\Omega=0$ and $\Omega=1$, present the same behavior as a function of J, but they differ significantly in magnitude with respect to each other and with respect to the results obtained for $j=0$. However, when averaged over the initial Ω the results for $j=0$ and $j=1$ become quite similar. This indicates that the difference arises from the stereodynamics. The reaction probabilities for specific values of Ω can be summed over J to obtain the helicity-dependent cross sections.[40] The fact that both the reaction probabilities and

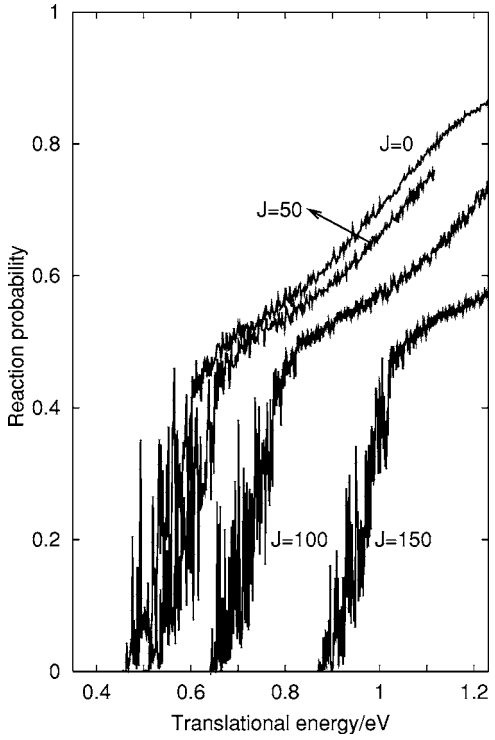

FIG. 4. Reaction probabilities in Ca+HCl($v=0, j=0$) collisions for several J values.

the helicity-dependent cross sections are larger for $\Omega=1$ implies that the reaction is more favored when the angular momentum **j** of the HCl reactant is initially parallel to the relative velocity vector **k**.

For $J>0$ the body-fixed xz plane rotates in space. Some more intuitive considerations can be made, however, if we place ourselves in the body-fixed frame. The distribution of the wave packet over the angle γ between the Jacobi vectors **r** and **R** is proportional $\sin^2\gamma$ for $j=1$, $\Omega=1$ and to $\cos^2\gamma$ for $j=1$, $\Omega=0$. Hence, the reaction turns out to be more favored when the two Jacobi vectors are initially perpendicular. Such a feature can be explained by the fact that the transition state is close to 60°, so that the reaction is more easily achieved for a perpendicular approach. These considerations are similar to those obtained from a stereodirected

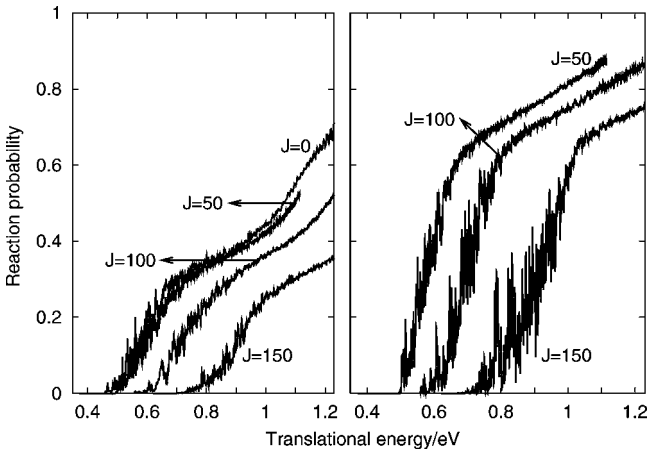

FIG. 5. Reaction probabilities in Ca+HCl($v=0, j=1$) collisions with $\Omega=0$ (left panel) and $\Omega=1$ (right panel) for several J values.

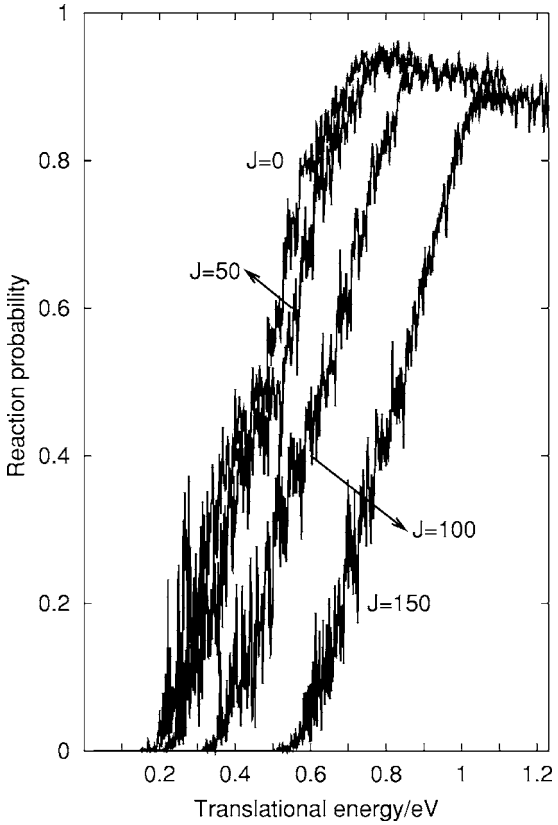

FIG. 6. Reaction probabilities in Ca+HCl($v=1, j=0$) collisions for several J values.

representation[57] or from the preferred attack angle method.[58] These methods use the complete S matrix for $J=0$ and were applied to Li+HF reactive collisions.

The reaction probability obtained for Ca+HCl collisions behaves oppositely to the reaction probability in the Li+HF system, in spite of the fact that the saddle points in both systems have a similar configuration, 57° for CaHCl and 75.5° for LiHF. In Li+HF($v=0$) collisions the reaction is more efficient when **j** and **k** are initially perpendicular or, in the rotating body-fixed frame, when initially **r** is parallel to **R**. This situation in LiHF was explained by the late nature of the barrier; to overcome the barrier some vibrational excitation of HF is needed, which is more easily obtained in nearly collinear collisions. For Li+HF($v=1$) the reaction probability is very high and nearly isotropic. That is, it does not depend on Ω, because a single vibrational quantum in the HF stretch is sufficient to produce the reaction with high efficiency.

To check whether similar vibrational effects are found for Ca+HCl, which also has a late barrier, we performed calculations for Ca+HCl($v=1, j$) collisions with initial $j=0$ and 1. The results are shown in Figs. 6 and 7. The major differences are that for $v=1$ the reaction probability above the threshold reaches 1 much faster and that the threshold is shifted to lower energies, by ≈ 0.2 eV. The location of the threshold is difficult to define precisely, but its shift from $v=0$ to $v=1$ is consistent with (but not equal to) the vibrational energy of HCl, that is, ≈ 0.37 eV. The reaction probabilities for $v=1$ are very similar for $j=0$ and $j=1$. Moreover, in the case of $j=1$ the reaction probabilities are not very different for $\Omega=0$ and 1. The only clear difference is that the energy shift for $J>0$ with respect to $J=0$ is larger for $\Omega=0$, since the rotational barrier in the CS approach is proportional to $J(J+1)-2\Omega$.[2]

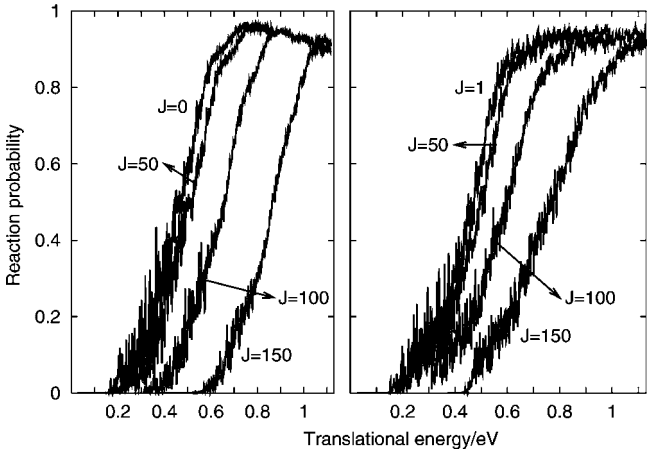

FIG. 7. Reaction probabilities in Ca+HCl($v=1, j=1$) collisions with $\Omega=0$ (left panel) and $\Omega=1$ (right panel) for several J values.

Hence, in Ca+HCl($v=1$) collisions the reaction probability is isotropic, i.e., it does not depend on Ω. This was also found for $v=0$ collisions at higher energies, and the reaction probabilities for $v=0$ and $v=1$ are nearly the same at equal total energies. The dependence of the reaction efficiency on Ω occurs only at low energies for Ca+HCl($v=0$) collisions, near the threshold. This stereodynamic effect is therefore attributed to the small angular cone of acceptance. The probability to reach this narrow acceptance cone depends on the initial orientation of reactants. However, at higher energies the cone opens to a rather wide angular region, so that the reaction efficiency no longer depends on the initial orientation. This effect is a function of the total energy, independent of whether vibrational or translational energy is provided.

In Li+HF collisions the reaction efficiency for $v=1$ is isotropic, while for $v=0$ it depends strongly on Ω. This feature is similar to what is found here for CaHCl, although the reaction is more efficient for lower Ω in LiHF and more efficient for higher Ω in CaHCl. Another difference in Li+HF collisions is that the efficiency for $v=1$ is significantly larger than for $v=0$ at the same total energy. This important dependence on the vibrational mode was explained by the late character of the barrier. In Li+HF one single vibrational quantum of HF is sufficient to pass over the barrier. When HF is in $v=0$ this excitation is more efficiently obtained in nearly collinear collisions, when it is in $v=1$ the reaction can occur directly.

Since both cases discussed, Ca+HCl and Li+HF, have a late barrier it is useful to determine what is the reason of this large difference in the dependence of the reaction on initial vibrational excitation. It may be argued that in CaHCl the HCl vibration is more excited during the approximation of the reactants, because the vibrational frequency is lower than that of HF. However, the interactions in the reactant channel are stronger in LiHF, so this seems not to be the reason.

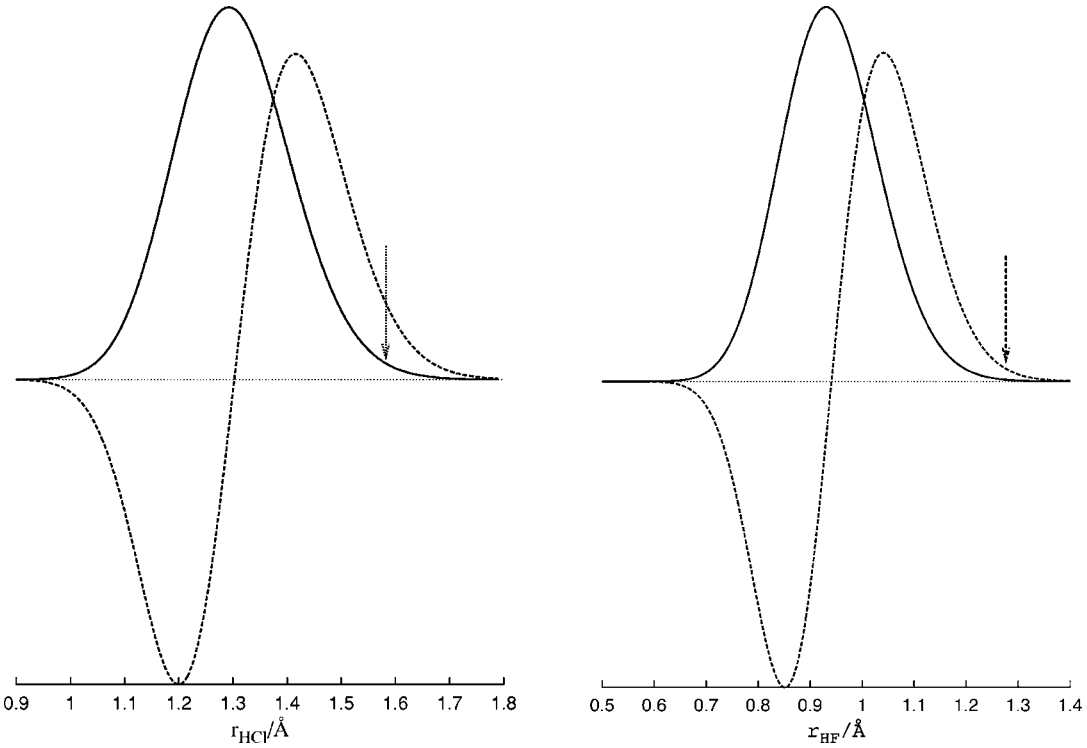

FIG. 8. Vibrational wave functions of free HCl(v=0,1), left panel, and HF(v=0,1), right panel. In both cases the position of the saddle point in the reactive PES is indicated with an arrow.

Another way to explain the difference is to somehow quantify the "late barrier character" of the reaction by considering the wave functions of the diatomic reactant in the initial vibrational state. The v=0 and v=1 wave functions of isolated HCl and HF are shown in Fig. 8. The arrows in this figure mark the HX bond lengths at the saddle point of the reaction. If the saddle point is located where the wave function has significant amplitude, the reaction will occur. This happens for HCl(v=0,1) and HF(v=1). Otherwise, if the amplitude is negligible, the reaction is enhanced by initial vibrational excitation of the reagent. This is observed for HF(v=0).

The orientational aspects of the reaction can be related to the angular cone of acceptance. If it is large, there is no significant dependence on the relative orientation of the initial **j** with respect to the relative velocity vector **k**. However, for low energies where the cone of acceptance is narrow, the reaction efficiency will depend on the relative orientation of **j** and **k**, in a way that is determined by the reaction mechanism.

The reaction probabilities have been calculated for $J=|\Omega|$ as well as for 50, 100, and 150, for different v, j, and Ω. The reaction probabilities for intermediate values of J were interpolated using a method based on the J-shifting approach,[56] which works very well in this case. The cross sections thus obtained, in Fig. 9, show a monotonous increase with translational energy, all with very similar slope. The reaction seems to be slightly enhanced when increasing j. The reaction cross section reaches nearly the same values for all initial states at the same total energy, except for $v=j=0$, where it seems to be slightly lower.

IV. PHOTOINITIATED DYNAMICS

An alternative way to study the reaction dynamics and probe the transition state region is through infrared excitation

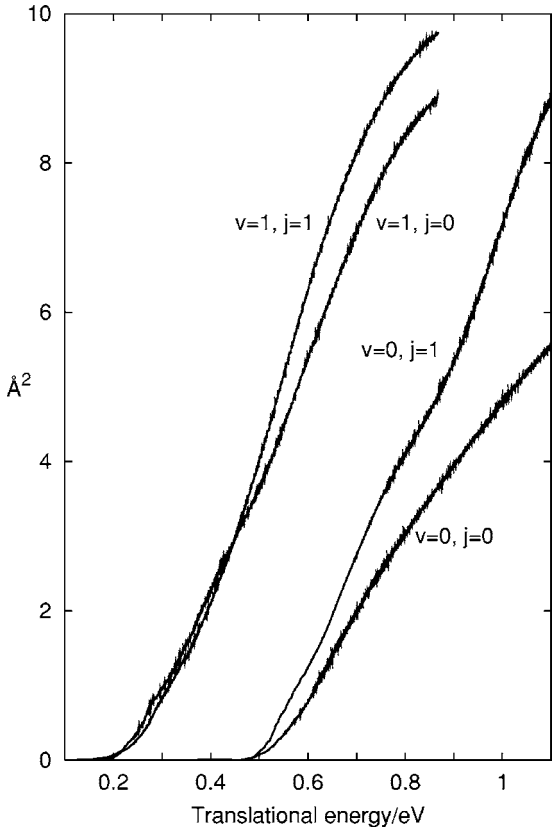

FIG. 9. Total reaction cross sections obtained for Ca+HCl(v,j) collisions.

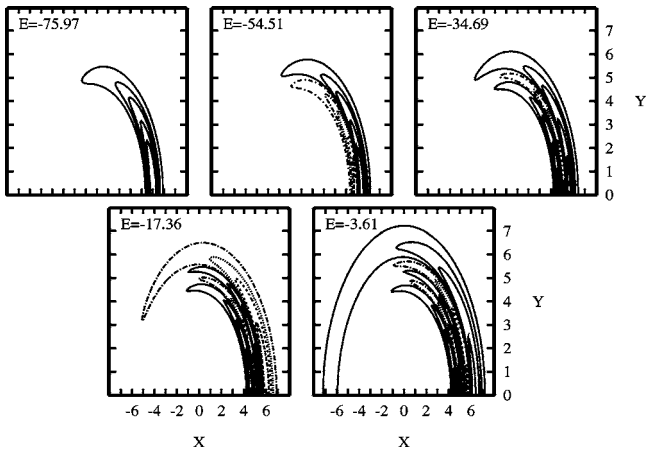

FIG. 10. Wave-function amplitudes for $J=0$ of the lower bound states in the Ca–HCl van der Waals well, for r frozen at its equilibrium value. The coordinates $X=R\cos\gamma$ and $Y=R\sin\gamma$ are in angstroms. The eigenvalues (in cm^{-1}) relative to Ca+HCl($v=0$) are given in each panel.

from the van der Waals well in the reactant valley. Such a study was performed for LiHF,[41] and it was found that an electric dipole infrared transition in the ground electronic state essentially produces an excitation of the HF mode. Since this mode is the reaction coordinate, the excited wave packet yields products with very high efficiency. For LiHF, the spectrum thus obtained corresponds to broad bands with a reaction probability close to one. For LiDF, however, the spectrum consists of several narrow peaks associated with resonances, because the excitation reached an energy region around the top of the barrier. The analysis of such resonances allows the characterization of the barrier for the reaction.

A similar study is of interest for CaHCl. The three main differences between the CaHCl and LiHF systems are the height of the barrier, much higher in CaHCl, the depth of the van der Waals well, deeper in LiHF, and the angular configuration of the well, located at $\gamma=0°$ for CaHCl and at $\gamma=110°$ for LiHF. After promotion from the van der Waals well, CaHCl dissociation dynamics will have more difficulty to yield the reaction products than in the LiHF case. The Ca–HCl complex has the advantage, however, of being more easily formed experimentally, since the reaction cross sections are zero at low translational energies.

The wave functions of some bound states in the van der Waals well of CaHCl are shown in Fig. 10. The van der Waals well is so shallow that it only supports few bound states. The lowest excited states, the energies of which are listed in Fig. 10, correspond to vibrational excitations in the R coordinate. Because the well is shallow and not very anisotropic and the zero-point energy is large, all bound states exhibit a substantial spreading in the angular coordinate γ.

In order to simulate the infrared spectrum, these initial states should be multiplied by the electric dipole transition operator, as described in Ref. 41. The electric dipole function used was obtained in Ref. 38. The two components of the electric dipole, in Fig. 11, present a smooth behavior as a function of the nuclear coordinates, with the z component parallel to the **R** vector being the largest. Transitions that are parallel with respect to this quantization axis are thus expected to dominate.

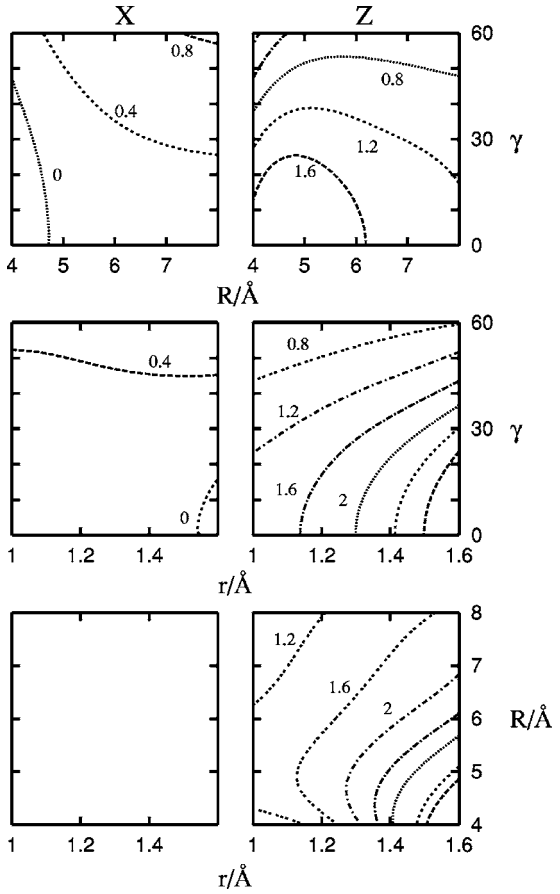

FIG. 11. Components of the electric dipole moment of Ca–HCl in the vicinity of the van der Waals well, from Ref. 38. Left (right) panels correspond to $x(z)$ body-fixed components. In the top panels r was fixed at 1.27 Å, in the middle panels R was fixed at 5.25 Å, and in the bottom panels $\gamma=0$.

An initial wave packet is built to study the $J=0\leftarrow 1$ rotational transitions from the ground van der Waals level. This wave packet, which is the product of the ground vibrational wave function of Ca–HCl, a rotational wave function with $J=1$, and the dipole function, may be decomposed into the vibrational states of bare HCl. It was found that the $v=0$ component is dominant, and that the weight decreases fast with increasing v. The component with $v=0$ corresponds to bound states that do not evolve in time. The components on higher v's dissociate, forming either unreacted Ca+HCl or CaCl+H reaction products.

The bound and slowly dissociating components of the wave packet require very long propagation times. In addition, a large energy interval had to be considered because of the different vibrational components of the wave packet, and the calculation of the complete spectrum at once requires very short time steps. Exact wave-packet calculations become prohibitively expensive. In order to overcome this problem, the wave packet was partitioned into different vibrational components[59] by projecting it onto the rovibrational functions of bare HCl, and each of these components was propagated independently. Such a procedure is formally approximate, but if the energy intervals of the different portions do not overlap each other, it can be considered essentially exact.[59] In the present case this is the situation. We

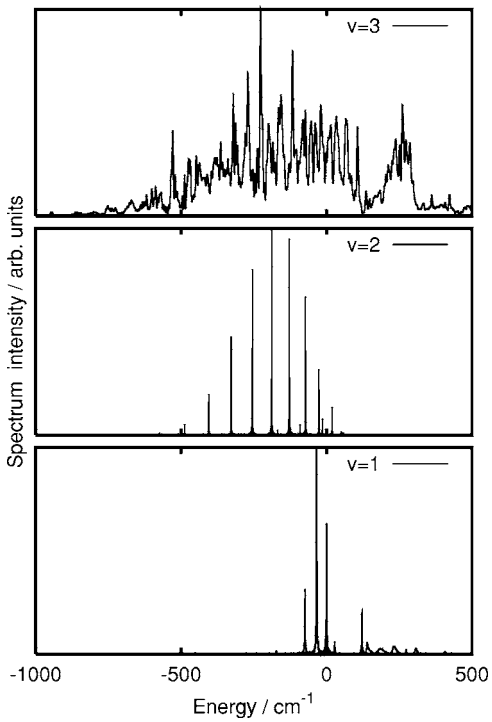

FIG. 12. Absorption spectra for the $v=1$, $v=2$, and $v\geqslant 3$ components of the wave packet, in the bottom, middle, and top panels, respectively. In each case the zero of energy is the corresponding HCl(v) asymptotic energy. In the cases of $v=1$ and $v=2$ the spectra have been obtained by multiplying the autocorrelation function by an exponential factor, with $\Gamma=1$ and 0.2 cm^{-1}, respectively (see text for details).

partitioned the initial wave packet into four portions: one for $v=0$, one for $v=1$, one for $v=2$, and the fourth one for all higher v collectively. It should be mentioned that the oscillator strength for excitation of the higher vibrational states is very small. The relative weights of the initial portions are 1.8% for $v=1$, 0.05% for $v=2$, and 0.0001% for $v\geqslant 3$.

Spectra were obtained by taking the Fourier transform of the autocorrelation function obtained in the wave-packet calculation. They are shown in Fig. 12. For the case of $v\geqslant 3$, the total spectrum was also obtained by summing the product fluxes in all rovibrational states of both HCl and CaCl, which served as a double check of the accuracy of the calculations. Such a check was not possible for $v=1$ and $v=2$, because the dissociation is very slow and it was not possible to collect the total flux.

The spectrum obtained for $v=1$, in Fig. 12, shows narrow peaks below zero and broader structures above this threshold. The zero of energy is defined as the energy of HCl($v=1$). All these structures are below the reaction barrier and below the energy of the products, and no flux towards CaCl+H products is obtained. The peaks above zero correspond to resonances in the continuum of Ca+HCl($v=0$), which are probably orbiting or rotational predissociation resonances with relatively short lifetimes. Below zero, however, the only dissociation pathway is through vibrational predissociation into Ca+HCl, which is very slow. In order to characterize the lifetimes of these vibrational predissociation resonances time-independent close-coupling (TICC) calculations[60,61] were performed. In these calculations we used reactant Jacobi coordinates, which is justified by the absence of reactivity at these energies. The results are listed in Table I. The very long lifetimes, on the order of milliseconds, could not possibly have been resolved through wave-packet calculations. The spectrum in Fig. 12 was obtained from wave-packet calculations by multiplying the autocorrelation function with an exponential damping function $\exp(-\Gamma t/\hbar)$, with $\Gamma=1$ cm^{-1}, in order to obtain a smooth spectrum. Thus, the widths of the peaks below zero were artificially enlarged. The structures above zero were not affected because they correspond to much faster processes.

TABLE I. Labels (i), energies (E), widths (Γ), and lifetimes (τ) of resonances appearing in the infrared spectra, as obtained from the time-independent close-cloupling method (see text and references for more details). The energies are relative to a particular vibrational Ca+HCl(v) asymptote denoted by v; they are the same as in Fig. 12.

v	i	E (cm^{-1})	Γ (cm^{-1})	τ (ps)
1				
	0	−172.365	2.68×10^{-6}	9.89×10^{5}
	1	−120.544	1.37×10^{-5}	1.94×10^{5}
	2	−74.752	1.72×10^{-5}	1.54×10^{5}
	3	−35.110	2.13×10^{-5}	2.13×10^{5}
2				
	0	−658.621	0.005 38	493.39
	1	−569.635	0.026 62	99.70
	2	−482.908	0.039 69	66.87
	3	−401.474	0.048 32	62.72
	4	−324.830	0.043 46	61.07
	5	−253.362	0.046 06	57.63
	6	−187.503	0.041 65	63.73

The situation for the $v=2$ spectrum in Fig. 12 is quite different. In this case, the energy is well above the CaCl($v=0$)+H threshold. However, the flux towards CaCl+H products obtained is negligible for all the spectral peaks, even when at the final time considered ($\approx$100 ps) an important portion of the wave packet has been absorbed at the edges of the grid. It is difficult to understand the low reactivity. The configuration of the Ca–HCl van der Waals complex is collinear while the saddle point is at angle $\gamma=67°$, and this large difference could be a reason. As in the case of $v=1$, the only dissociation pathway that is then left for these resonances is vibrational predissociation, which would justify why these resonances are so long lived. TICC calculations were performed. The lifetimes found, shown in Table I, are on the order of several hundreds of picoseconds.

What is remarkable is the important change in the absorption spectrum in comparison with that for $v=1$. For $v=2$ the peaks are shifted towards lower energies by about 500 cm^{-1} with respect to the corresponding HCl($v=2$) asymptote. A redshift is commonly observed in the diatom bound levels of atom-diatom van der Waals clusters, but the frequency shifts are usually much smaller. The extremely large shift observed here, larger than the van der Waals well depth of $\approx$200 cm^{-1}, is explained by the opening of the product channel. We illustrate this point by showing in Fig. 13 the PES of CaHCl weighted with the square of the vibrational wave functions of HCl for $v=0$, 1, and 2. The plots

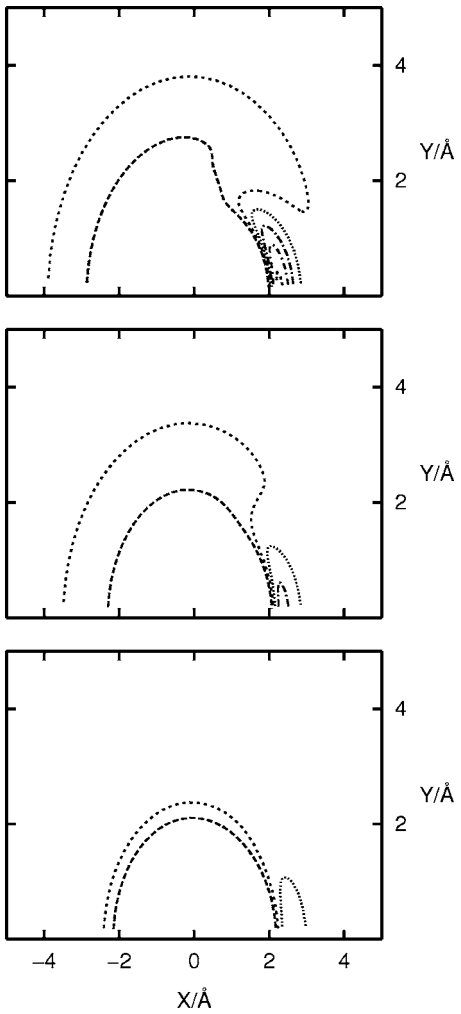

FIG. 13. Potential-energy surface of CaHCl weighted by the squared HCl(v=0, 1, and 2) vibrational wave functions. The contours are −700, −500, −300, −100, 100, and 300 cm^{-1}, all relative to the corresponding HCl(v) asymptotic energy.

show deep wells, consistent with the energy levels associated with the peaks of the spectra in Fig. 12. As the vibrational excitation of HCl increases, the wave functions obtain significant amplitude for larger HCl bond lengths. As can be seen in Fig. 8, the HCl(v=1) wave function has an amplitude around the saddle point. Even larger distances are reached for v=2, so that the wave function can explore configurations near the deep insertion minimum, at the other side of the reaction barrier.

There was an apparent disagreement between the theoretical value of approximately 200 cm^{-1} for the dissociation energy of Ca–HCl from *ab initio* calculations[38] and the empirical estimate[13] of approximately 1000 cm^{-1}. de Castro-Vítores *et al.*[13] considered two major contributions, one arising from van der Waals interactions, of ≈200 cm^{-1}, and one due to a charge-transfer contribution. This last contribution was added to match the experimentally estimated dissociation energy of Menéndez *et al.*[62] The latter estimate was based on the energetics of a reactive collision experiment, in which the product recoil energy was neglected. On the basis of the present results it may be considered that the Ca–HCl van der Waals complex formed in the experiments of Soep and co-workers[17–20] is not bound, but corresponds to one or several of these long-lived resonances, which have dissociation energies up to ≈650 cm^{-1} with respect to the corresponding HCl(v) asymptote. The latter value of the Ca–HCl binding energy would explain the formation of Ca–HCl complexes in competition with Ca_2 dimer formation.[63] Also the charge-transfer contribution to the binding energy would then be justified. The reaction barrier is the result of a curve crossing between covalent and ionic states, and the deep well after the barrier corresponds to an ionic $H^-Ca^{2+}Cl^-$ insertion complex.[38] However, in the experimental setup the van der Waals complexes formed must live at least several hundreds of microseconds before being excited,[63] while the calculated resonances have lifetimes on the order of nanoseconds. The lifetimes are extremely sensitive to details of the barrier, though, and small changes in the height, width, or shape of the calculated barrier may perhaps produce sufficiently long-lived resonances. Given the difficulties mentioned in Ref. 38 in accurately describing the heavy Ca atom, such changes cannot be excluded. New *ab initio* calculations address this point.

The resonance structure associated with each peak in Fig. 12 was studied with the use of a pseudospectral method,[41] and by the calculation of (quasi)bound states on the two-dimensional PES shown in Fig. 13 for v=2. Each of these bound states corresponds to a v=2 excitation in the HCl vibration, but they have different quantum numbers (n,b) associated with the Ca–HCl stretch and bend. Two progressions are observed and assigned, as noted in Fig. 12. The main one is attributed to a vibrational progression in the Ca–HCl stretch mode, with the bend in its ground level centered around the collinear geometry. The first peak, at −575 cm^{-1}, is already singly excited in the Ca–HCl stretch. The energy separation between peaks decreases from 90 to 46 cm^{-1} due to the large anharmonicity of the PES. In the second progression, again with varying stretch quantum number, all levels are in the first bend excited mode. The first peak of appreciable intensity at −168 cm^{-1} already corresponds to three quanta in the stretch mode.

Finally, the spectrum associated with the $v \geqslant 3$ band in Fig. 12 occurs at energies similar to those for v=2 [relative to the corresponding HCl(v) asymptotes], but there are more and much broader resonances. The large increase of the width or, alternatively, the large decrease in lifetime, is explained by the increase of anharmonic coupling, leading to vibrational predissociation towards Ca+HCl, and the effective opening of the reaction channel towards CaCl+H products. As is shown in Fig. 14, the reaction probability associated with the $v \geqslant 3$ band is on the order of 50%.

This finding is analogous to the results obtained for LiHF and LiDF.[41] The advantage of CaHCl, besides that the complex is more easily formed because it is nonreactive at low temperatures, is that one may study the gradual opening of the reaction channel by increasing v. A problem is the low oscillator strength to directly excite the $v \geqslant 3$ manifold. However, since intermediate resonances belonging to v=1 and even v=2 manifolds have very long lifetimes, it should be possible to promote the system in two steps.

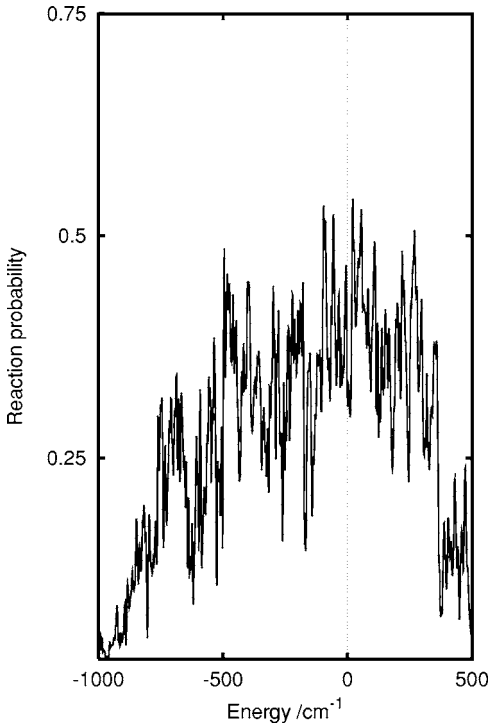

FIG. 14. Probability of forming CaCl+H products for the band corresponding to $v \geqslant 3$ in Fig. 12; energy relative to HCl($v=3$).

V. CONCLUSIONS

The reaction dynamics of Ca+HCl→CaCl+H in its ground electronic state was studied with the use of a wave-packet method. We used a recently proposed PES (Ref. 38) which has a late barrier, at a HCl bond length somewhat larger than the HCl equilibrium distance. The height of the barrier is 0.4 eV, the energy of the CaCl+H products is 0.46 eV. In the product channel, after the barrier, is a deep insertion well of ≈2 eV. However, the reaction seems to follow a direct mechanism. Only when the energy is near the threshold some resonances appear.

The effect of vibrational and rotational excitations of the reactants was investigated; we observed only small changes of the total reaction cross sections. The small effect of vibrational excitation is surprising, because of the late character of the reaction barrier. It is contrary to the large effect observed for the Li+HF reaction, which has a late barrier also. The difference is explained by the fact that, in contrast with Li +HF, the initial wave function for HX($v=0$) does not vanish at the geometry of the saddle point. There is a significant stereodynamic effect for Ca+HCl($v=0$), which disappears for $v=1$, because of the increase of the angular cone of acceptance.

The barrier for the reaction is the result of an ionic/covalent curve crossing. It has been probed in this work by simulating infrared excitation from the Ca–HCl van der Waals well in the reactant valley. The frequency of the HCl stretch mode is much larger than that of the other vibrational modes and the spectrum can be separated into several bands, or groups of peaks, which belong to particular vibrational states v of HCl. It was found that the spectra up to $v=2$ vibrational excitation of HCl consist of narrow resonances. The only fragmentation mechanism is vibrational predissociation, while the reaction probability is still negligible. Even for $v=2$, although the energy is already above the reaction threshold. The binding energies (up to ≈650 cm^{-1}) of these resonant states of Ca–HCl with respect to the corresponding v level of HCl are considerably larger than the van der Waals well depth of ≈200 cm^{-1}. The explanation of this remarkable feature is that the vibrational wave function of HCl extends to considerably larger distances with increasing v, and samples the region of the deep insertion well that lies directly beyond the barrier in the product channel.

The formation of these long-lived and stable resonances found especially for $v=2$ could also reconciliate the *ab initio* calculated value[38] of about 200 cm^{-1} for the binding energy of the Ca–HCl complex with the much larger value estimated experimentally.[62] That is, if one assumes that the latter value actually corresponds to one or more of these resonances. The experimental setup would require longer lifetimes than we found in this paper, but these lifetimes are extremely sensitive to details of the barrier that are hard to calculate with sufficient accuracy. It should also be noted that the larger Ca–HCl binding energy in the experimental estimate is entirely due to a charge-transfer contribution that is not found in the *ab initio* calculated Ca–HCl van der Waals well, but is present in the resonances. The reason is that these resonances sample the insertion well, which corresponds to the ionic species $H^-Ca^{2+}Cl^-$.

The Ca–HCl infrared spectrum corresponding to $v \geqslant 3$ excited HCl shows many overlapping broad resonances. The simulated reaction probability is approximately 50% in this case. We may therefore conclude that a spectroscopic study through infrared excitation from the van der Waals well will provide detailed information about the reaction barrier, from energies where no reaction occurs up to energies well above the saddle point. Moreover, it may be possible to form the very stable HCaCl insertion complex through such transitions, by an indirect mechanism that passes through a long-lived resonance with substantial amplitude in the insertion well.

In a subsequent study, which is in progress, we model the Ca+HCl reaction dynamics in excited electronic states. Experimentally this is studied both by collisions[8–16] and through electronic excitation of the Ca atom in the van der Waals complex in the reactant channel.[17–20] Here, we expect nonadiabatic effects to be more important than in the ground state and we include multiple-coupled potential-energy surfaces.

ACKNOWLEDGMENTS

We would like to acknowledge Professor B. Soep, Professor M. Paniagua, Professor A. Aguado, Dr. G. Verbockhaven, and Dr. T. González-Lezana for very fruitful discussions. This work has been supported by MEC (Spain), under Grant No. CTQ2004-02415.

[1] D. R. Herschbach, Adv. Chem. Phys. **10**, 319 (1966).
[2] J. C. Polanyi and W. H. Wong, J. Chem. Phys. **51**, 1439 (1969).
[3] M. H. Mok and J. C. Polanyi, J. Chem. Phys. **51**, 1451 (1969).

[4] R. D. Levine and R. B. Bernstein, *Molecular Reaction Dynamics and Chemical Reactivity* (Oxford University Press, Oxford, 1987).
[5] J.-M. Mestdagh, B. Soep, M.-A. Gaveu, and J.-P. Visitcot, Int. Rev. Phys. Chem. **22**, 285 (2003).
[6] H. Eyring and M. Polanyi, Z. Phys. Chem. Abt. B **12**, 279 (1931).
[7] J. L. Magee, J. Chem. Phys. **8**, 687 (1940).
[8] U. Brinkmann and H. Telle, J. Phys. B **10**, 133 (1977).
[9] H. Telle and U. Brinkmann, Mol. Phys. **39**, 361 (1980).
[10] U. Brinkmann, V. H. Schmidt, and H. Telle, Chem. Phys. Lett. **73**, 530 (1980).
[11] C. T. Rettner and R. N. Zare, J. Chem. Phys. **75**, 3636 (1981).
[12] C. T. Rettner and R. N. Zare, J. Chem. Phys. **77**, 2416 (1982).
[13] M. de Castro-Vítores, R. Candori, F. Pirani, V. Aquilanti, M. Garay, and A. González-Ureña, Chem. Phys. Lett. **263**, 456 (1996).
[14] M. Garay, C. A. Rinaldi, J. M. Orea, and A. González-Ureña, Chem. Phys. Lett. **236**, 343 (1998).
[15] M. de Castro-Vítores, R. Candori, F. Pirani, V. Aquilanti, M. Garay, and A. González-Ureña, J. Phys. Chem. A **102**, 9537 (1998).
[16] M. Garay, J. M. Orea, A. González-Ureña, and G. Roberts, Mol. Phys. **97**, 967 (1999).
[17] B. Soep, C. J. Whitham, A. Keller, and J. P. Visticot, Faraday Discuss. Chem. Soc. **91**, 191 (1991).
[18] B. Soep, S. Abbés, A. Keller, and J. P. Visticot, J. Chem. Phys. **96**, 440 (1992).
[19] A. Keller, R. Lawruszczuk, B. Soep, and J. P. Visticot, J. Chem. Phys. **105**, 4556 (1996).
[20] R. Lawruszczuk, M. Elhanine, and B. Soep, J. Chem. Phys. **108**, 8374 (1998).
[21] C. A. Mims, S.-M. Lin, and R. R. Herm, J. Chem. Phys. **57**, 3099 (1972).
[22] J. G. Pruett and R. N. Zare, J. Chem. Phys. **64**, 1774 (1976).
[23] Z. Karny and R. N. Zare, J. Chem. Phys. **68**, 3360 (1978).
[24] Z. Karny, R. C. Estler, and R. N. Zare, J. Chem. Phys. **69**, 5199 (1978).
[25] A. Siegen and A. Schultz, J. Chem. Phys. **72**, 6227 (1980).
[26] C.-K. Man and R. C. Estler, J. Chem. Phys. **75**, 2779 (1981).
[27] A. Torres-Filho and J. G. Pruett, J. Chem. Phys. **77**, 740 (1982).
[28] A. Torres-Filho and J. G. Pruett, J. Chem. Phys. **77**, 1774 (1982).
[29] R. Zhang, D. J. Rakestraw, K. G. McKendrick, and R. N. Zare, J. Chem. Phys. **89**, 6283 (1988).
[30] R. L. Jaffe, M. D. Pattengill, F. G. Mascarello, and R. N. Zare, J. Chem. Phys. **86**, 6150 (1987).
[31] A. J. H. M. Meijer, G. C. Groenenboom, and A. van der Avoird, J. Phys. Chem. A **101**, 7558 (1997).
[32] M. de Castro-Vítores, R. Candori, F. Pirani, V. Aquilanti, M. Garay, and A. González-Ureña, J. Chem. Phys. **112**, 770 (2000).
[33] M.-Q. Cai, L. Zhang, B.-Y. Tang, M.-D. Chen, G.-W. Yang, and K.-L. Han, Chem. Phys. **255**, 283 (2000).
[34] A. D. Isaacson and J. T. Muckerman, J. Chem. Phys. **73**, 1729 (1980).
[35] J. L. Schreiber and P. J. Kuntz, J. Chem. Phys. **76**, 1872 (1982).
[36] C. Sanz, O. Roncero, C. Tablero, A. Aguado, and M. Paniagua, J. Chem. Phys. **114**, 2182 (2001).
[37] M. J. McGuire, P. Piecuch, K. Kowalski, S. A. Kucharski, and M. Musia, J. Phys. Chem. A **108**, 8878 (2004).
[38] G. Verbockhaven, C. Sanz, G. C. Groenenboom, O. Roncero, and A. van der Avoird, J. Chem. Phys. **122**, 204307 (2005).
[39] A. Aguado, M. Paniagua, M. Lara, and O. Roncero, J. Chem. Phys. **107**, 10085 (1997).
[40] M. Lara, A. Aguado, O. Roncero, and M. Paniagua, J. Chem. Phys. **109**, 9391 (1998).
[41] M. Paniagua, A. Aguado, M. Lara, and O. Roncero, J. Chem. Phys. **111**, 6712 (1999).
[42] R. N. Zare, *Angular Momentum* (Wiley, New York, 1988).
[43] H. Tal-Ezer and R. Kosloff, J. Chem. Phys. **81**, 3967 (1984).
[44] C. Leforestier, R. H. Bisseling, C. Cerjan *et al.*, J. Comput. Phys. **94**, 59 (1991).
[45] M. Lara, A. Aguado, M. Paniagua, and O. Roncero, J. Chem. Phys. **113**, 1781 (2000).
[46] A. Aguado, M. Paniagua, C. Sanz, and O. Roncero, J. Chem. Phys. **119**, 10088 (2003).
[47] W. H. Miller, J. Chem. Phys. **61**, 1823 (1974).
[48] D. H. Zhang and J. Z. H. Zhang, J. Chem. Phys. **101**, 3672 (1994).
[49] D. Neuhauser, J. Chem. Phys. **100**, 9272 (1994).
[50] E. M. Goldfield, S. K. Gray, and G. C. Schatz, J. Chem. Phys. **102**, 8807 (1995).
[51] A. Aguado, M. Paniagua, M. Lara, and O. Roncero, J. Chem. Phys. **106**, 1013 (1997).
[52] G. G. Balint-Kurti, R. N. Dixon, and C. C. Marston, J. Chem. Soc., Faraday Trans. **86**, 1741 (1990).
[53] S. K. Gray and G. G. Balint-Kurti, J. Chem. Phys. **108**, 950 (1998).
[54] Y. Xhang, T.-X. Xie, K.-L. Han, and J. Z. H. Zhang, J. Chem. Phys. **119**, 12921 (2003).
[55] T.-S. Chu and K.-L. Han, J. Phys. Chem. A **109**, 2050 (2005).
[56] J. M. Bowman, Adv. Chem. Phys. **61**, 115 (1985).
[57] J. M. Alvariño, V. Aquilanti, S. Cavalli, S. Crocchianti, A. Laganà, and T. Martínez, J. Phys. Chem. A **102**, 9638 (1998).
[58] M. P. Miranda, S. Crocchianti, and A. Laganà, J. Phys. Chem. A **103**, 10776 (1999).
[59] O. Roncero, J. Campos-Martínez, M. I. Hernández, G. Delgado-Barrio, P. Villarreal, and J. Rubayo-Soneira, J. Chem. Phys. **115**, 2566 (2001).
[60] O. Roncero, J. A. Beswick, N. Halberstadt, P. Villarreal, and G. Delgado-Barrio, J. Chem. Phys. **92**, 3348 (1990).
[61] F. X. Gadéa, H. Berriche, O. Roncero, P. Villarreal, and G. Delgado-Barrio, J. Chem. Phys. **107**, 10515 (1997).
[62] M. Menéndez, M. Garay, E. Verdasco, and A. González-Ureña, J. Chem. Soc., Faraday Trans. **89**, 1493 (1993).
[63] B. Soep (private communication).